

pubs.acs.org/Macromolecules Article

Ester Side Chain Functionalization Enhances Mechanical Properties of Poly(3-Hexylthiophene) while Maintaining High Hole Mobility

Quynh D. Tran, Lexi R. Knight, Guanchun Rui, Gage T. Mason, Piumi Kulatunga, Alexander J. Bushnell, Buwei Hou, Lei Zhu, Simon Rondeau-Gagné, and Geneviève Sauvé*



Cite This: Macromolecules 2024, 57, 4544-4555



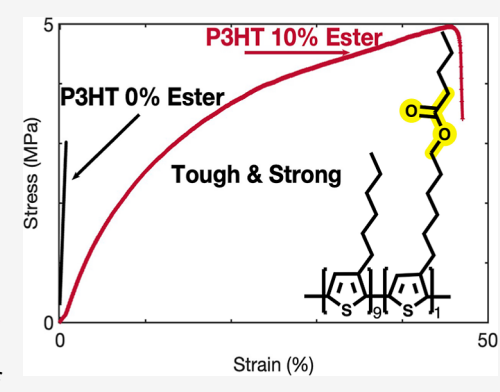
ACCESS I

III Metrics & More

Article Recommendations

sı Supporting Information

ABSTRACT: Regioregular poly(3-alkylthiophene)s (P3AT) are easy to synthesize conjugated polymers with good electrical properties, but they tend to be brittle, limiting their application. To improve their mechanical properties, we investigated incorporating ester groups in the side chains of P3AT six carbons away from the polymer backbone. Two random copolymer series were synthesized: poly(3-alkylthiophene-2,5-diyl)-ran-(3-(6-pentanoatehexyl)thiophene-2,5-diyl), where the alkyl is either *n*-hexyl (P3HT series) or *n*-dodecyl (P3DDT series). In both the series, the ester-functionalized side chain had a length similar to that of *n*-dodecyl and its content was varied from 0 to 100 mol %. The copolymer's optical, thermal, structural, electrical, and mechanical properties were investigated. The effect of 10–25% ester content on copolymer film aggregation behavior was very different for each series: for the P3HT series, the side chains cocrystallized with the main chains into one crystal structure and behaved as one phase. As a result, incorporation of



the longer ester-functionalized side chain greatly affected the thermal, morphological, and mechanical properties. For the P3DDT series, the side chains and main chains crystallize separately, and the n-dodecyl and ester-functionalized side chains appear to cocrystallize together. As a result, the main chain melting temperature decreases only slightly with the ester content, and the mechanical properties were not significantly improved with 10-25% ester. The best combination of mechanical robustness and charge carrier mobility was thus obtained for the P3HT random copolymer with $\sim 10\%$ ester: a high fracture strain ($29 \pm 6\%$) combined with a high tensile strength (3.9 ± 0.6 MPa) resulted in a large toughness (90 ± 30 J/m³). This was achieved while maintaining the same high charge carrier mobility as P3HT of similar molecular weight (0.12 ± 0.01 cm² V⁻¹ s⁻¹). Improved ductility was also shown by the thin film-on-elastomer technique. These results demonstrate that side chain modification can optimize both the mechanical and electrical properties of P3ATs when the side chains and the main chain behave as one phase.

■ INTRODUCTION

Conjugated polymers (CPs) are integrated into a wide range of organic electronic applications, such as organic photovoltaics (OPVs), organic light-emitting diodes (OLEDs), and organic field-effect transistors (OFETs).^{1–4} Some advantages of organic electronics include flexibility, lightweight, low cost, chemical tunability, and solution-processing capability.^{5,6} In addition, self-healing, biodegradability, biocompatibility, and other new functionalities can be incorporated into CPs via rational design of the chemical structure, expanding CPs toapplications such as biomedical devices for health monitoring purposes.^{6–9}

To enable organic electronics, a lot of effort has been devoted to optimizing charge carrier mobility, but less attention has been devoted to optimizing mechanical properties, which is critical for flexible devices. In these materials, charge transport is achieved via intrachain conjugation or interchain π – π stacking. To maximize charge transport, increasing the planarity of the polymer conjugated backbone is critical to both extend the conjugation length and facilitate

interchain hopping. As a result, high performance CPs tend to be highly crystalline or semicrystalline, which results in brittle materials with high stiffness. ^{11,12} This restricts their use in rigid or semiflexible device applications and limits device lifetime due to cracking. ¹³ More flexible and ductile materials can be obtained if the microstructure is more amorphous, which allows rotational and conformational freedom for polymer chains to realign and reorganize to dissipate mechanical stress. ¹⁴ However, these tend to have lower charge carrier mobility, thus making it challenging to optimize both the charge transport and mechanical properties. Very high molecular weight (MW) CPs can have good charge transport properties while being more stretchable due to the long-

Received: September 15, 2023 Revised: March 29, 2024 Accepted: April 15, 2024 Published: April 23, 2024





intertwined polymer chains that 'connect' crystalline regions within the film. However, it is not often practical to synthesize very high MW CPs due to solubility issues or polymerization terminations.

Several alternative strategies have been explored to improve the mechanical properties of CPs. Extrinsic approaches include the use of additives, such as triacetin, to improve stretchability of CPs in OFETs, or blending CPs with nonconjugated polymers that have the desired mechanical properties. 16-18 A second approach is to improve the intrinsic properties of CPs via rational design of the chemical structure such as backbone or side chain engineering. Examples of chemical structure modification include introducing nonconjugated spacers, dynamic covalent bonds such as hydrogen- or metal-ligand bonding, controlling polymer sequence such as alternating, random, or block copolymers, and adding large and flexible side chains. 5,13 Recent efforts have been successful in creating highly flexible CPs with high charge carrier mobility in FETs, ideally suited for applications that interface with biology. Less work has been reported on CPs that have high flexibility and high tensile strength, i.e., tough or robust CPs, which would be suited for robust electronic devices such as sensors, LEDs, or OPVs. 13 Even more elusive are CPs that are flexible and elastic, meaning they return to their original shape after stretching. There is therefore a great need for more structure-property studies to better understand how to tune the mechanical properties of CPs while maintaining good electrical properties.

Regioregular poly(3-alkylthiophene)s (P3ATs) are an important class of CPs that are simple to synthesize, have been extensively studied, and have good electrical properties. $^{19-22}$ Like many CPs, they tend to be brittle. The most common P3AT, poly(3-hexylthiophene) (P3HT), is no exception. For a relatively high MW that is still relatively easy to solution-process (Mn \sim 95 kDa), tensile-strain tests of free-standing films show that it is brittle with a fracture strain of only 0.7% and tensile strength of 3.0 MPa. 23 Efforts to improve the mechanical properties of P3AT include adding very large flexible side chains and making random copolymers with thiophenes. 8,23 Very little is known about the introduction of simple functional groups in the side chain of P3ATs.

In a previous study, we modified the side chains of P3HT to increase its dielectric constant, as shown in Figure 1.24 To our surprise, P3 has unusual properties for a P3AT: it formed freestanding films that could be handled by hand. The stressstrain curve of a thick free-standing film, Figure 1b, shows that P3 is tough with a high tensile strength of 5 MPa and a high fracture strain of ~25%. Unfortunately, P3 has very poor electrical properties since it is 100% functionalized. Since these improvements in mechanical properties were not seen in P2, we hypothesize that they were caused by the ester group, perhaps due to its flexible nature and its ability to have dipole dipole interactions. Interestingly, many plasticizers contain ester groups.²⁵ In addition, ester-functionalization was recently used to improve fracture strain of poly[(2,6-(4,8-bis(5-(2ethylhexyl-3-chloro)thiophen-2-yl)-benzo[1,2-b:4,5-b']dithiophene))-alt-(5,5-(1,3'-di-2-thienyl-5',7'-bis(2-ethylhexyl)benzo[1',2'-c:4',5'-c']dithiophene-4,8-dione))] (PM7) from 20% to 47–58%.²⁶ The authors wrote that the flexible ester side chains provide pathways for relaxation against applied stresses compared to rigid units in PM7, though the ester groups also affected polymer backbone planarity since they are directly connected to the polymer backbone. In the case of P3ATs, ester-functionalized copolymers where the ester

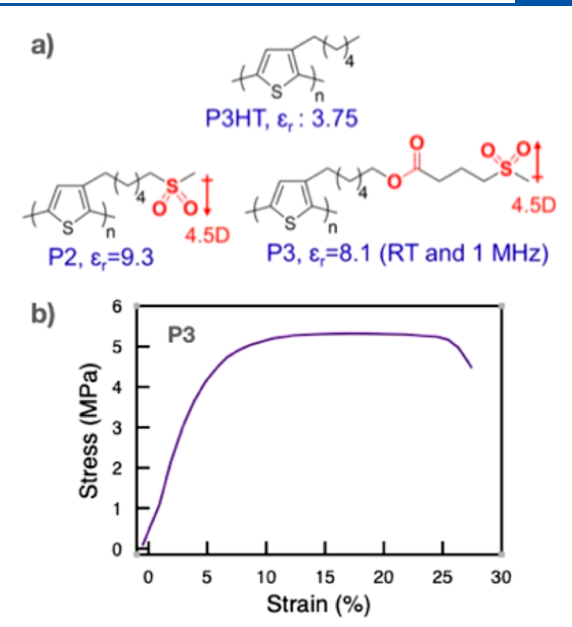


Figure 1. (a) Polymer structures and dielectric constants; (b) stress—strain curve of P3 obtained by DMA in tensile mode from free-standing films.

group is adjacent to the conjugated polymer were found to improve electrical properties and stretchability. There is a study where ester groups were introduced further from the polymer backbone and integrated into OPVs, but no mechanical properties were reported. To the best of our knowledge, no investigation of the effect of ester groups on electrical and mechanical properties when placed further away from the polymer backbone, such as in P3, was reported.

To verify our ester hypothesis, we first synthesized P3ATs similar to P3 but without a sulfone group. However, the 100% functionalized polymer is gooey and has bad electrical properties. To establish the ester content that simultaneously optimizes mechanical and electrical properties, we varied the ester content from 0 to 100%. A very simple way to vary the ratio of two monomers is using random copolymers; we therefore synthesized copolymers that randomly combined ester-functionalized 3-alkylthiophene with 3-alkylthiophene, as depicted in Scheme 1.²⁴ Since little is known about the effect of simple functional groups in P3ATs, we questioned whether the alkyl side chain should be shorter or of similar length as the ester functionalized side chain. Since the ester group is six carbons away from the polymer backbone, we investigated nhexyl (P3HT series) where the alkyl is shorter than the esterfunctionalized side chain and n-dodecyl (P3DDT series) where the alkyl is the same length as the ester-functionalized side chain, as shown in Scheme 1. The copolymers were obtained using a previously reported method, where random copolymers of 3-alkylthiophene and 3-(6-bromohexyl)thiophene with desired ratios are first synthesized using the Grignard Metathesis (GRIM) method, see Scheme 2.24 The brominated side chains are then converted to esters via postpolymerization reactions with pentanoic acid.²⁴ The repeating units of the polymers were kept low (35-45 repeating units) to maintain a high solubility in organic solvents and to limit entanglement effects. The copolymer's thermal, optical, structural, mechanical, and electronic properties were investigated. This systematic study revealed that ~10% ester content improves the mechanical properties of P3ATs without negatively impacting

Scheme 1. Random Copolymers Containing an Ester Functional Group Within the Side Chains: P3HT and P3DDT series. X:Y is the Non-functionalized Monomer: Ester Functionalized Monomer Feed Ratio. Note: the 8:1 Ratio Corresponds to 11 mol % Ester, which We Rounded Down to 10% for Simplicity

Scheme 2. Reaction Scheme of P3AT Copolymers

the electronic properties. Further, the effect of the ester group on mechanical properties is maximized when the coalkyl side chain is shorter (*n*-hexyl).

■ RESULTS AND DISCUSSION

Synthesis. Random copolymers of 3-alkylthiophene and 6-bromo-3-hexylthiophene were synthesized using GRIM (Scheme 2), following the published methods. ^{24,30} The ratio of nickel catalyst to monomer was adjusted to obtain a relatively low molecular weight, which is important to maintain optimal polymer solubility in organic solvents for postpolymerization reactions. We aimed for a number of repeating units of about 40. The actual numbers of repeating units (or the degree of polymerization DPn) were estimated from ¹H NMR using end-group analysis and were between 31 and 45, averaging ~37 (see Table S1). ³⁰ Molecular weights were also estimated by gel permeation chromatography in THF using polystyrene

standards. The $M_{\rm w}$ ranged between 7 and 14 kDa (see Table S2 and Figures S27 and S28). The copolymers actual mole % of 6-bromoalkyl thiophene was estimated by ¹H NMR spectroscopy using the peak integration from methyl protons at 0.9 ppm and the methylene protons adjacent to the Br at 3.42 ppm, see Table S3. The experimental mole % functionalization obtained was very similar to the theoretical values calculated from the monomer ratios. The desired esterfunctionalized random copolymers were obtained by postpolymerization reaction of the 6-bromo-3-hexyl side chains with pentanoic acid in high yields (Scheme 2).²⁴ Complete conversion to ester functionality was confirmed by ¹H NMR with the disappearance of the peak at 3.42 ppm and the appearance of triplet peaks at 2.29 and 4.06 ppm (Figures S18-S26). In addition, we confirmed that there was no Fsubstitution in the resulting ester random copolymers by the

absence of two triplets at 4.41 and 4.52 ppm (H_{α} on F-substitution).

Optical Properties. The polymers' UV–vis absorption spectra in solution are given in Figure 2, and the λ_{max} values are

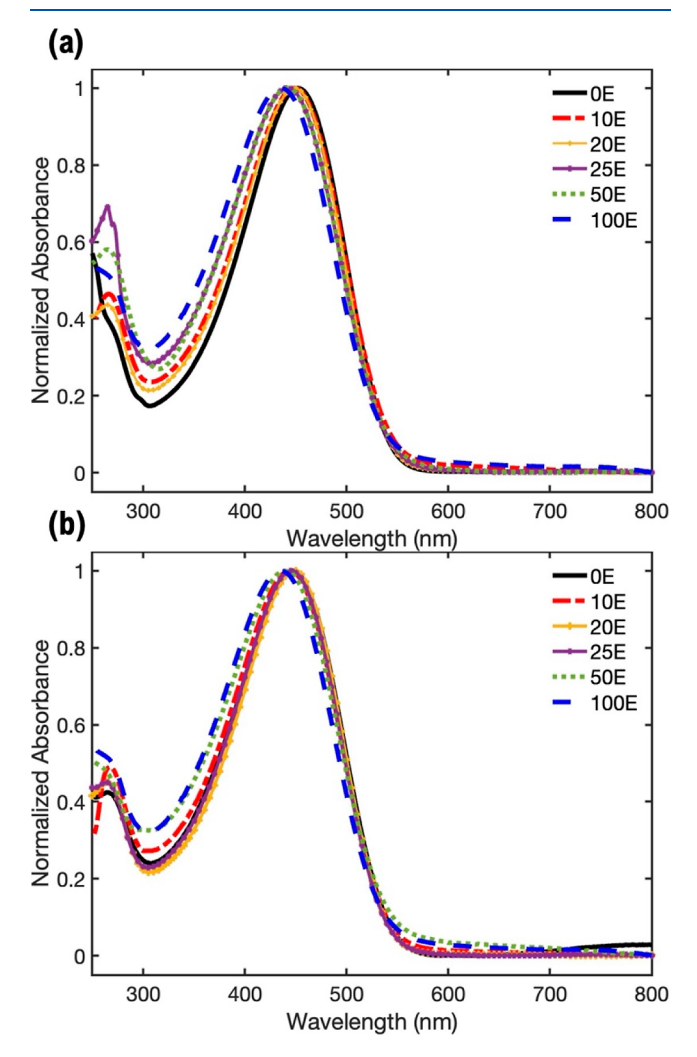


Figure 2. UV-vis absorption spectra of (a) P3HT and (b) P3DDT series in solution.

summarized in Table 1. All absorption spectra are very similar, with a small blue shift from P3HT (452 nm) and P3DDT (447 nm) to the 100% ester functionalized polymer ($\lambda_{max} = 436$ nm). The minimal effect of the ester groups on the absorption

spectra in solution is as expected since the ester group is several carbons from the conjugated backbone.

The UV-vis absorption spectra for the as-cast and annealed films are shown in Figure 3, and the optical properties are summarized in Table 1. The main visible absorption peak for all polymers red shifts upon film formation by 61-77 nm for 0-50% ester and by 49 nm for the 100% ester polymer, indicative of extended π -conjugation in films. The 0–50% ester-containing polymers also show the typical vibronic shoulders for P3AT films, which generally become a bit more pronounced upon annealing 125 °C for 15 min. The vibronic shoulders indicate some aggregation and π – π stacking in the films. In the P3HT series, the incorporation of ester functionalized side chains decreases the vibronic shoulders, as would be expected with increased disorder due to the random incorporation of the longer ester-functionalized side chain. In the P3DDT series, however, the vibronic shoulders appear to be stronger for the 10–25% ester copolymers than for P3DDT, suggesting that some ester functionality helps aggregation and π - π stacking. At ~50% ester content, however, the vibronic shoulders become less pronounced than those of P3DDT, and the 100% ester polymer spectrum does not show any vibronic shoulders. Further, annealing the 100% ester polymer film significantly blue shifts the absorption by 44 nm to 441 nm, becoming like the solution spectrum (436 nm). The ester groups in P3DDT-100E therefore thermodynamically discourage planarization and $\pi - \pi$ stacking. The optical band gap values for the polymers were estimated from the absorption onset, λ_{onset} , and were all ~1.9 eV, except for P3DDT-100E, which has a higher optical band gap of 2.18 eV.

Thermal Properties. The polymers' thermal properties were evaluated by thermogravimetric analysis (TGA) and differential scanning calorimetry (DSC). The TGA thermograms are shown in Figure S31, and the temperature values at 5% weight loss $(T_{d,5})$ are summarized in Tables S4 and S5. The decomposition of all copolymers occurs in one step around 400 °C, comparable to P3HT and P3DDT homopolymers. This contrasts with a study from Son et al. showing that degradation of ester side chains occurs in two steps forming carboxylate at 200 °C and complete removal of the carboxylate group at 300 °C. 31 The difference is in the placement of the ester group: our copolymers have the ester group in the middle of the side chain, whereas the polymers with lower degradation temperatures have the ester group next to the thiophene. We concluded that placing the ester groups in the middle of the side chain did not lead to degradation at lower temperatures.

Table 1. Summary of Optical Properties of P3AT Copolymers in Solution and Film

polymer	λ_{\max} solution (nm)	$\lambda_{ ext{max}}$ as-cast (nm)	solution to film shift (nm)	$\lambda_{ ext{max}}$ annealed $(ext{nm})$	as-cast to annealed shift (nm)	$\lambda_{ m onset}$ annealed film (nm)	$\frac{E_{\mathrm{opt}}}{(\mathrm{eV})}$
P3HT (0E)	452	522	70	520	-2	643	1.93
10E	449	515	66	506	-9	646	1.92
20E	448	520	72	514	-6	644	1.93
25E	441	502	61	494	-8	643	1.93
50E	448	520	72	514	-6	641	1.93
P3DDT (0E)	447	521	67	498	-12	649	1.91
10E	443	520	77	515	-5	651	1.90
20E	448	523	75	516	- 7	651	1.90
25E	446	519	73	502	-17	653	1.90
50E	439	504	65	490	-14	645	1.92
100E	436	485	49	441	-44	568	2.18

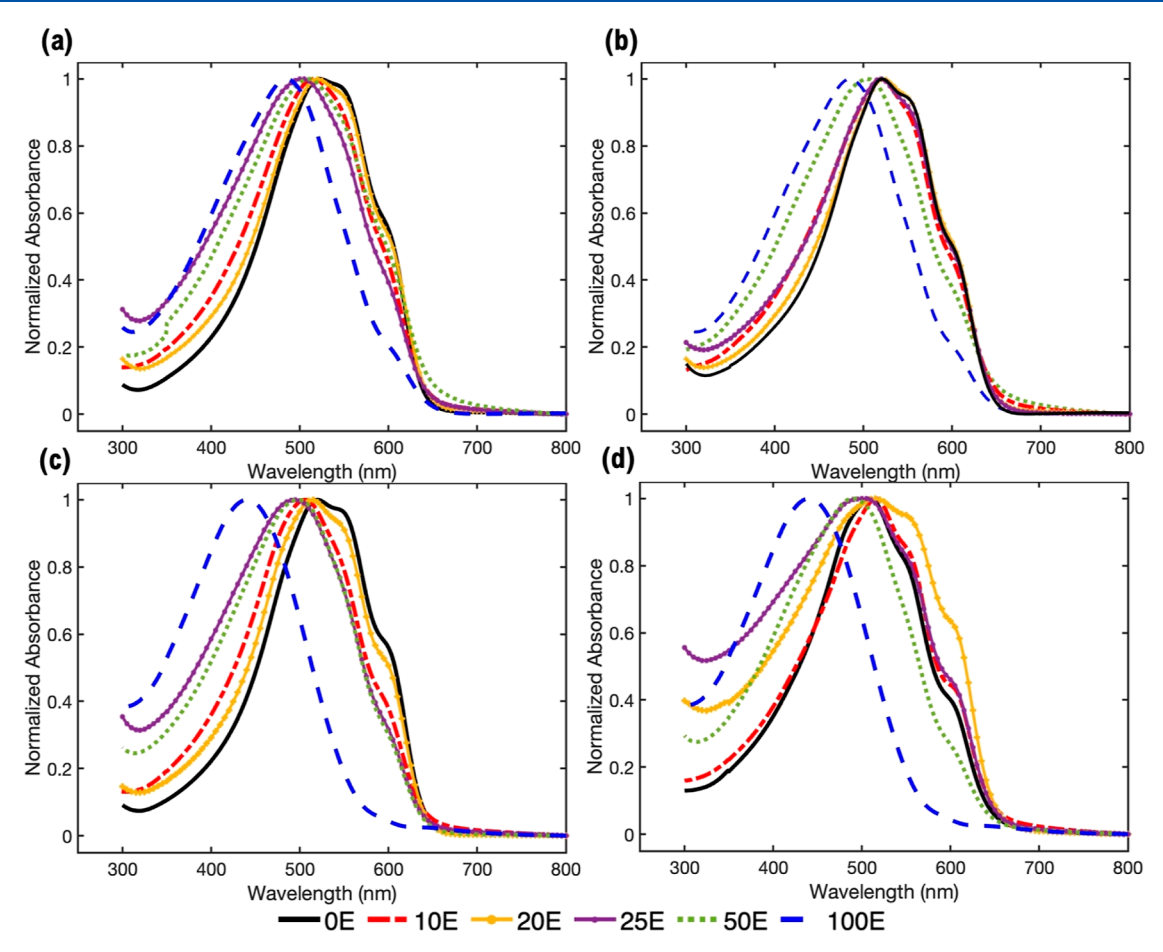


Figure 3. UV—vis absorption spectra of as-cast films for (a) P3HT and (b) P3DDT copolymers. UV—vis absorption spectra of annealed films for (c) P3HT and (d) P3DDT copolymers.

The DSC thermograms for the second heating and cooling cycles are shown in Figure 4, and the thermal events are summarized in Figure 5a,b and Tables S4 and S5. Both P3HT and P3DDT exhibit melting and crystallization peaks due to their semicrystalline nature. P3HT shows one sharp melting peak at 231 °C during the heating cycle and one sharp crystallization peak at 198 °C during the cooling cycle. The polymer melting temperature (T_m) and crystallization temperature decrease significantly with the ester content, see black dash line in Figure 4a,c, as well as Figure 5a These results indicate that ester-functionalized side chains strongly impact the polymer's intermolecular forces and tight packing in the solid state. The enthalpy of melting (ΔH_m) , which is determined from integration of the melting peak, also decreases with increasing ester content, see black curve in Figure 5B. This is consistent with ester groups decreasing the copolymer's crystallinity. P3DDT shows two melting peaks during the heating cycle, one at 68 °C and one at 145 °C. These are attributed to the side chain and main chain melting, respectively.³² Both the main chain and side chain recrystallize separately during the cooling cycle. Figure 5a shows that the side chain melting temperature (T_{m1}) and main chain melting temperature (T_{m2}) decrease with the ester content, but the decrease in $T_{\rm m2}$ with ester content is much less than what was observed for the P3HT series. Figure 5b shows that $\Delta H_{\rm m1}$ decreases with the ester content, but $\Delta H_{\rm m2}$ seems to fluctuate around 10 J/g. The $\Delta H_{\rm m2}$ for P3DDT-10E appears to be lower than P3DDT, whereas those for P3DDT-20E, -25E and -50E

are similar to that of P3DDT. We have repeated this measurement and currently cannot explain this inconsistency. It could be due to differences in sample history or impurities in the sample. The 100% ester polymer is very different than P3DDT despite having similar side chain lengths: it shows a small broad melting peak around 68 °C that could be attributed to main chain crystals and a small broad recrystallization peak around 15 °C during the cooling cycle, presumably related to main chain recrystallization. These results show that the ester groups have dramatic effects on the thermal properties.

Powder Wide-angle X-Ray Diffraction. The polymers' degree of crystallinity was estimated from the powder patterns shown in Figures S32 and S33 and summarized in Figure 5c. The percent crystallinity of P3HT was 55%, which is similar to the literature value.³³ The percent crystallinity decreased to 40% as the ester content increased to 50%, consistent with increased disorder due to side chain mismatch. Interestingly, the 100% ester polymer had a crystallinity higher than that of P3HT-50E, at ~52%, where the side chains are no longer mismatched. The unit cell dimensions for the a-axis (lamellar) and b-axis $(\pi - \pi)$ stacking are shown in Figure 5d. The $\pi - \pi$ stacking distance does not change with the ester content, but the lamellar distance increases linearly with ester content. This is due to the incorporation of the longer ester-functionalized side chain and is consistent with the side chain and main chain cocrystallizing and behaving as one phase. The trends are very different for the P3DDT series. The crystallinity of P3DDT

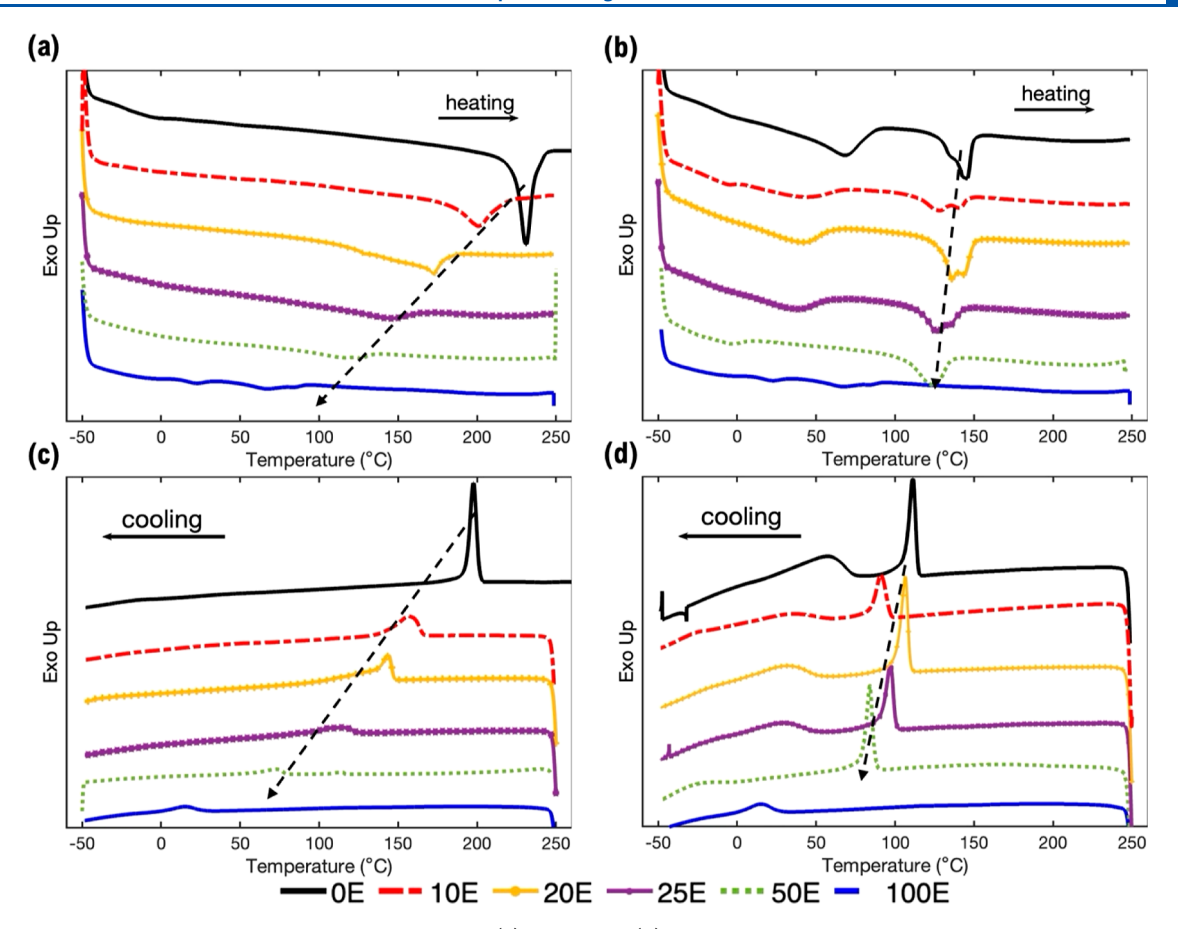


Figure 4. DSC thermograms showing the 2nd heating cycle of (a) P3HT and (b) P3DDT series. DSC thermograms shwong the 2nd cooling cycle of (c) P3HT and (d) P3DDT series. The black dashed lines are added to guide the eye.

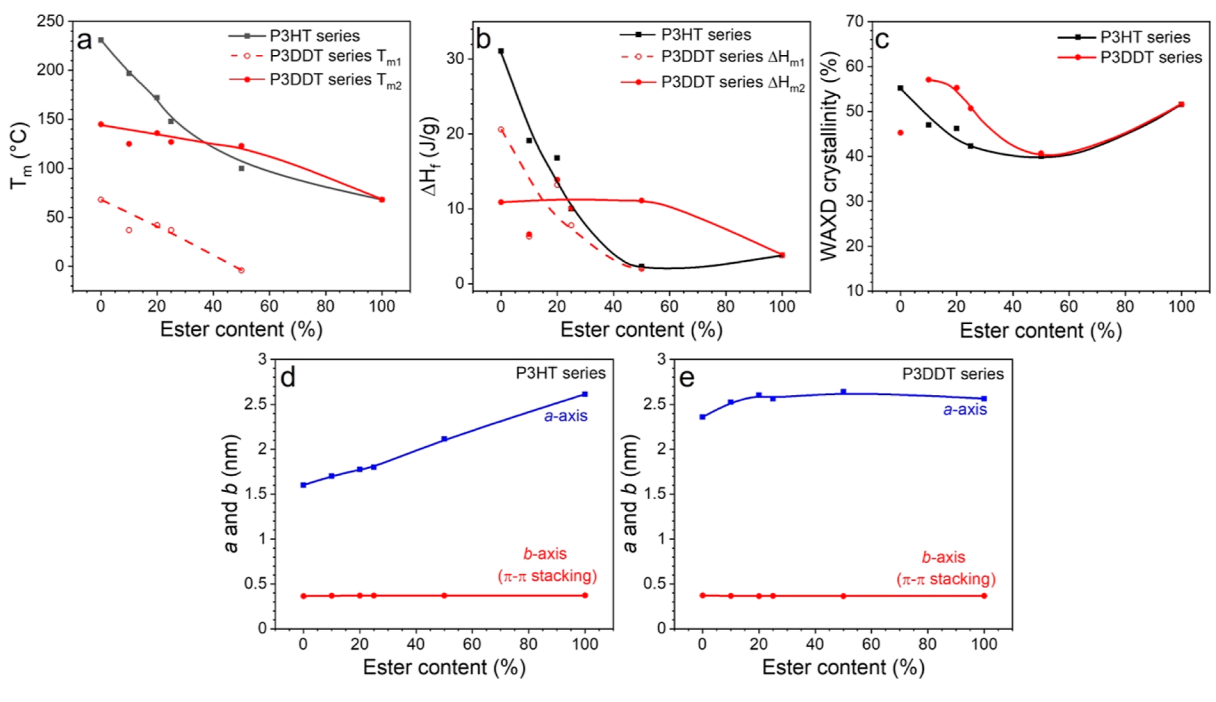


Figure 5. Summary of (a) $T_{\rm m}$ and (b) $\Delta H_{\rm m}$ for P3HT and P3DDT series. (c) Percent crystallinity as a function of ester content for the P3HT and P3DDT series. Unit cell dimensions a and b for the (d) P3HT and (e) P3DDT series. The lines are added to guide the eye.

was 45% and increased to 57% for P3DDT-10E. Some ester functionality may help crystallization due to dipole—dipole interactions. Further increasing the ester content decreases

crystallinity to 40% for P3DDT-50E. Note that P3HT-10E, -20E, and -25E all had higher relative crystallinity than P3DDT. Figure 5e shows that the π - π stacking distance (b-

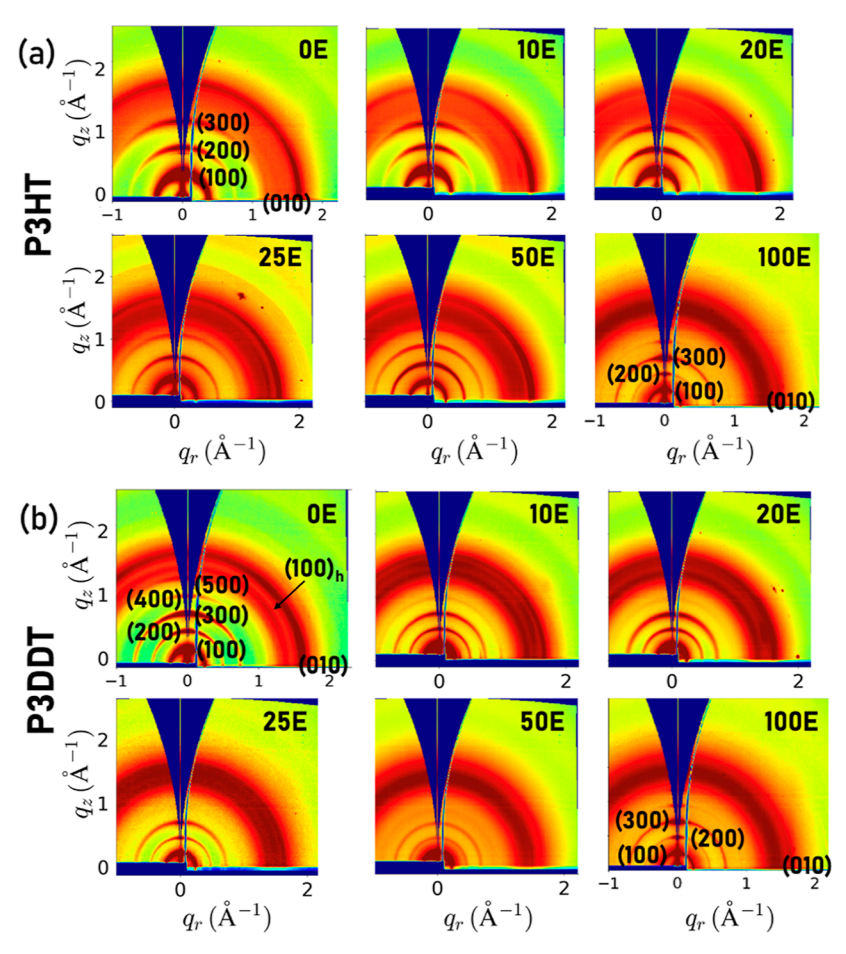


Figure 6. 2D GIWAXD images of P3HT (a) and P3DDT (b) series.

axis) does not change with the ester content. The lamellar distance (a-axis) increases only slightly when the copolymers have ester groups, consistent with the side chains being of similar length and possibly cocrystallizing together.

The DSC and powder WAXD data strongly suggest that for the P3HT series (0-50% ester), the side chains and the main chain cocrystallize as one phase. As a result, side chain modification strongly impacts the P3HT copolymer's thermal behavior. On the other hand, for the P3DDT series (0-50%), the longer *n*-dodecyl side chains crystallize separately from the main chain due to stronger van der Waals forces. This results in a microphase separation between the main chain and the side chains, as observed previously.³² Because the side chains and main chain are immiscible, it makes sense that the side chain modification would not strongly impact the main chain thermal behavior, as observed for the P3DDT copolymers. To verify this hypothesis, we performed heating WAXD experiments for both the P3HT and P3DDT series, as shown in Figures S34 and S35. For the P3HT series, the 1D WAXD profile during stepwise heating does not change until the temperatures reaches the melting point and the polymer melts. This is consistent with the main chain and side chain behaving as one phase. The situation for the P3DDT series is different since there are two melting temperatures, one for the side chain and one for the main chain. At a low temperature range (see Figure S35 for exact ranges), there are peaks for both the side chain (K_{SC}) and main chain (K_{MC}) and then a higher temperature range with only $K_{\rm MC}$ before the polymer melts. The mixed ester and *n*-dodecyl side chains possibly crystallize

together into one isomorphic crystal structure because the melting peak at low temperatures between 0 and 80 °C could not be deconvoluted into two melting peaks. Meanwhile, their crystal reflections could not be clearly identified in WAXD, suggesting relatively poor crystal-packing.

Thin Film Morphology. To better understand the influence of ester side chains on film morphology, grazingincident wide-angle X-ray diffraction (GIWAXD) was obtained for thermally annealed spin-coated thin films on silicon wafers. The 2D GIWAXD patterns are shown in Figure 6, and the corresponding intensities along the vertical (out-of-plane) and horizontal (in-plane) directions versus the scattering vector (q) plots are shown in Figure 7. The GIWAXD lamellar and π - π stacking distances are summarized in Table 2. The GIWAXD pattern for P3HT shows the characteristic P3HT diffraction peaks with lamellar reflections in the out-of-plane direction and π - π stacking in-plane, pointing to mainly edge-on orientation, though there is a significant amorphous content. As the ester content increases to 50%, the amorphous content increases, and orientation becomes poorer. The lamellar distance also increases from 16.6 Å for P3HT to 22.0 Å for P3HT 50E, consistent with the powder XRD data discussed above. The π - π stacking distance remains at ~3.7-3.8 Å for all copolymers.

The P3DDT polymer shows a diffraction pattern consistent with a mostly type I form, where the side chains are not interdigitated.^{34,35} The lamellar patterns can be seen in both the out-of-plane and in-plane directions, though the intensity is greater in the out-of-plane direction, pointing to a preference

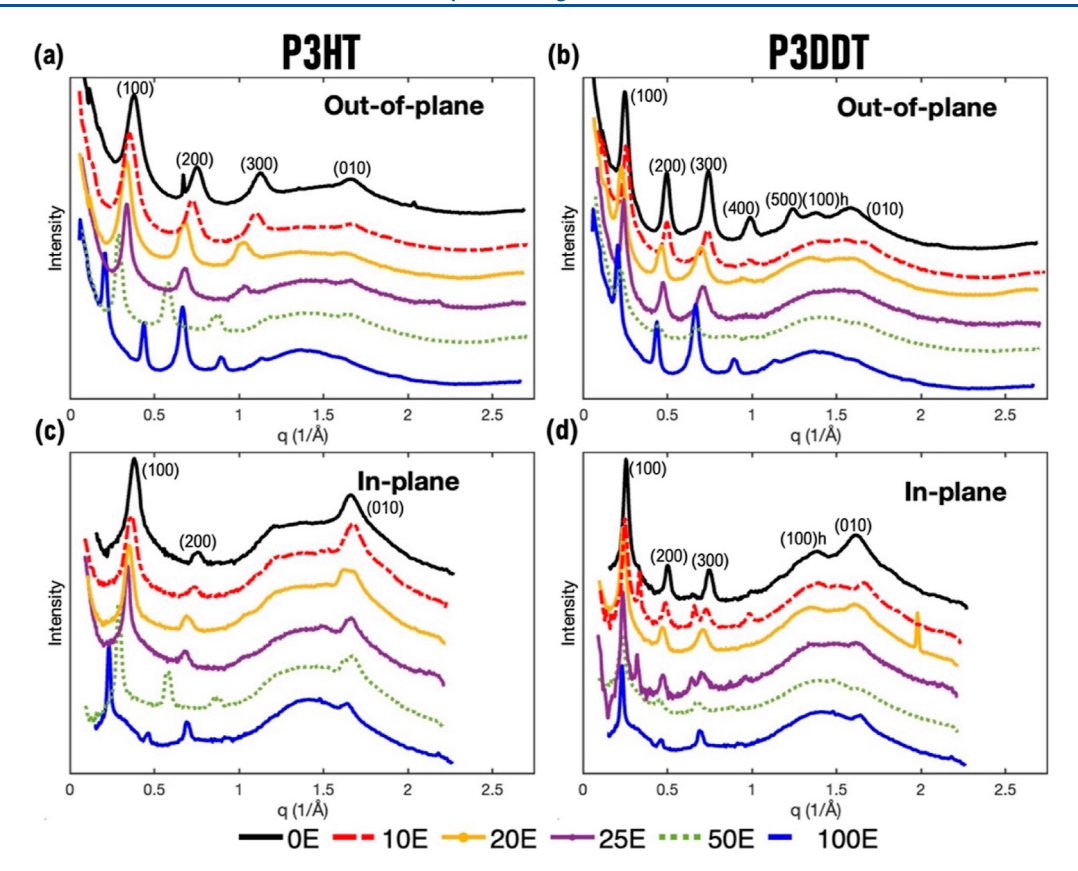


Figure 7. 1D GIWAXD intensity vs q plots for out-of-plane (top) and in-plane (bottom) for (a, c) P3HT and (b, d) P3DDT series.

Table 2. Summary of GIWAXD Lamellar and $\pi - \pi$ Distances

polymer	lamellar spacing (Å) type I (type II in-plane)	π - π (Å)
P3HT (0E)	16.6	3.8
10E	18.0	3.8
20E	18.8	3.9
25E	18.8	3.8
50E	21.7	3.8
P3DDT (0E)	25.4	3.9
10E	24.7 (19.0)	3.9
20E	27.9	3.9
25E	26.3 (19.0)	3.9
50E	28.4	3.9
100E	30.9	3.9

for the edge-on orientation with a significant amorphous component. The lamellar distance of 25.4 Å is slightly smaller than the reported type I (27.1 Å), but significantly larger than the more compact side-chain indigitated type II form (19.8 Å).³⁵ This observation is also consistent with the mostly type I form. A π - π distance of 3.9 Å could be calculated for the P3DDT copolymers; however, the intensity of the peak significantly decreased with 10% or higher ester functionalization. The lamellar distance increases from 25.4 Å for P3DDT to 31.0 Å for the 100% ester polymer, even though the two side chains are of the same length. This suggests that the ester groups push the lamellar stack farther away from each other. Interestingly, the P3DDT films with 10, 20, and 25% ester also have in-plane diffraction patterns with a lamellar spacing of 19.0 Å, consistent with a small amount of the type II form that is mainly face-on. This has also been observed in regionandom

P3DDT and could be possible because of the random nature of the copolymers³⁴ or small (unintentional) differences in film processing conditions. The 100% ester polymer shows a different set of lamellar peaks than P3DDT, with a larger lamellar distance of 30.9 Å that has mainly an edge-on orientation.

The P3DDT and P3DDT copolymers show an additional peak labeled $(100)_h$ (Figure 6b, 0E), which is attributed to side chain crystallization. This peak is calculated to be $\sim\!4.6$ Å, consistent with previous reports of P3DDT XRD where the side chains approximate a 4.5 Å hexagonal close packing. The side chain peak decreases in intensity as the ester content increases and completely disappears in P3DDT-50E. This suggests that the ester-functionalized side chains interfere with crystallization of n-dodecyl side chains.

The thin film surface morphology was imaged by atomic force microscopy (AFM, see Figures S36–S39). Generally, the 1 μ m \times 1 μ m images of all the polymers are very similar and show a relatively smooth surface with no clear formation of nanofibrils, even for the 100% P3HT sample. For the 5 μ m \times 5 μ m images, more defects were observed due to the larger scanning area. Furthermore, the 100% ester polymer appears to have a surface texture different from those of the other polymers, pointing to a very different self-assembly.

Mechanical Properties. To evaluate the mechanical properties of P3AT random copolymers, we fabricated thick (0.1–0.2 mm) free-standing films. This was achieved by dropcasting a 140 mg/mL P3AT solution in *o*-chlorobenzene onto a glass slide that was precoated with PEDOT:PSS. The PEDOT:PSS layer was then dissolved in water to give a free-standing P3AT film for tensile tests. Our P3HT, P3DDT, and P3DDT-100E homopolymers could not be tested because

adequate free-standing films could not be made: the P3HT and P3DDT films fractured when dissolving the PEDOT:PSS layer in water, and the P3DDT-100E was too sticky to be handled properly. For each copolymer, 4–7 samples were measured. Figure 8 shows stress—strain plots for the best sample of each

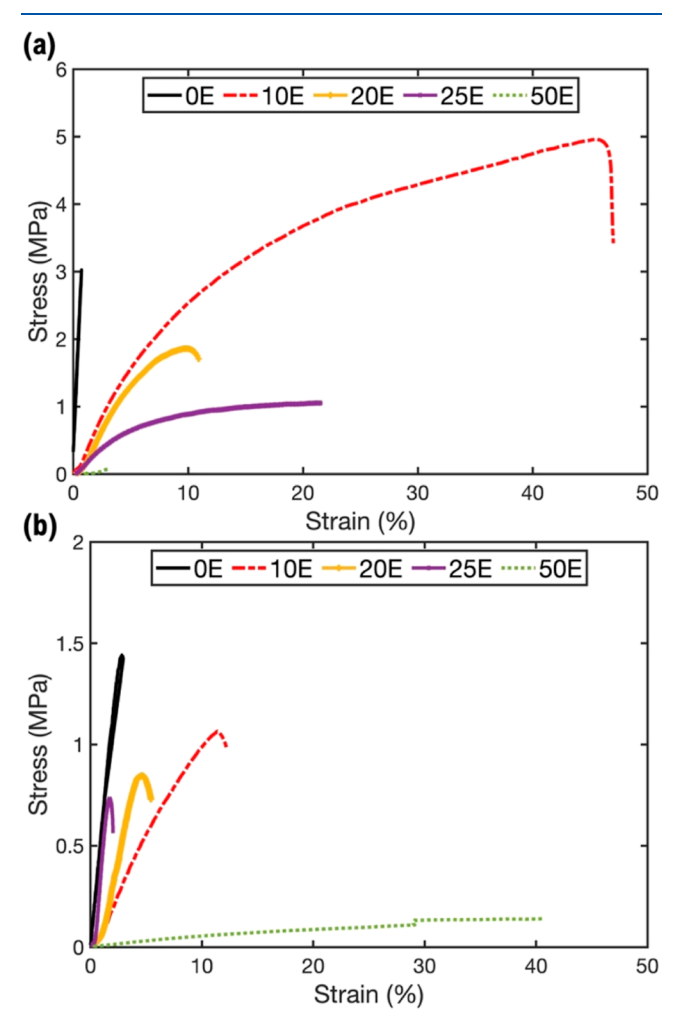


Figure 8. Stress-strain plots for the (a) P3HT and (b) P3DDT series.

copolymer. The corresponding parameter averages and standard errors are reported in Table 3 and plotted for visualization in Figure S40. For comparison, we also added data extracted from the literature for P3HT and P3DDT homopolymers.²³ Sydlik and co-workers were able to obtain tensile tests for free-standing films of P3HT and P3DDT, presumably because they have much higher MW than our polymers (PDn 95).²³ Higher MW values are known to improve robustness.

Compared to the reference P3HT, P3HT-10E has a much smaller elastic modulus, 46 MPa versus 350 MPa for high MW P3HT. P3HT-10E has a slightly higher tensile strength (3.9 MPa) and much larger fracture strain (29%) than the P3HT reference (3.0 MPa, 0.7% fracture strain, respectively), making it about 75 times tougher than P3HT (\sim 90 vs 1.2 J/m³). This is impressive considering that the reference P3HT has a higher MW than the P3HT-10E copolymer (DPn \sim 45 for our P3HT and P3HT-10E versus DPn \sim 95 for the reference P3HT). As the ester content increases to 50%, the elastic's modulus decreases to 6 MPa, consistent with ester functionalization

Table 3. Parameters Extracted From the Tensile Tests for P3HT and P3DDT Series

polymer	elastic's modulus (MPa)	tensile strength (MPa)	fracture strain (%)	toughness (J/m^3)
P3HT (0E)	350	3.0	0.7	1.2
10E	46 ± 6	3.9 ± 0.6	29 ± 6	90 ± 30
20E	32 ± 3	2.0 ± 0.2	11 ± 2	13 ± 3
25E	10 ± 2	0.7 ± 0.1	18 ± 1	9 ± 2
50E	6.3 ± 0.6	0.17 ± 0.03	4.2 ± 0.3	0.34 ± 0.07
P3DDT (0E)	55	1.4	2.8	2.2
10E	14 ± 0.4	0.95 ± 0.08	9 ± 1	5.1 ± 0.9
20E	23 ± 2	0.6 ± 0.1	3.6 ± 0.6	1.1 ± 0.3
25E	33 ± 9	0.45 ± 0.09	2.3 ± 0.4	0.5 ± 0.1
50E	0.8 ± 0.2	0.14 ± 0.04	26 ± 5	2.2 ± 0.7
100E	_	_	_	_

softening the free-standing films and making it more deformable. Tensile strength and fracture strain also decrease significantly with increasing ester content, going down to 0.17 MPa and 4.2% for 50% ester content, respectively. As a result, the random copolymer's toughness decreases with the ester content, going down to 0.34 J/m³ for 50% ester content. Despite this trend, the copolymers with 10%, 20%, and 25% ester content all have a higher toughness than the P3HT reference, which means they can absorb higher total mechanical stress than the P3HT reference. Of the P3HT series, 10% ester content resulted in the most robust copolymer.

The effects of the ester content on the mechanical properties of P3DDT are very different than those of P3HT (Figure 8b and S40, Table 3). The P3DDT-10E copolymer has a lower modulus, 14 ± 0.4 MPa vs 55 MPa for P3DDT. The P3DDT-10E also has a lower tensile strength (0.95 \pm 0.08 vs 1.4 MPa) and a higher fracture strength (9 \pm 1 vs 2.8%), resulting in a 2.5-fold increase in toughness (5.1 \pm 0.9 vs 2.2 J/m³ for the P3DDT reference). This increase in toughness is much more modest than what was observed for the P3HT-10E. As the ester content increases further, the elastic modulus slightly increases to 33 ± 9 MPa for 25% ester content and then significantly decreases to 0.8 ± 0.2 MPa for 50% ester content. Tensile strength decreases with ester content, down to 0.14 \pm 0.04 MPa for the P3DDT-50E, whereas fracture strain decreases to $2.3 \pm 0.4\%$ for 25% ester content and then significantly increases to $26 \pm 5\%$ for 50% ester content. As a result, toughness decreases to $0.5 \pm 0.1 \text{ J/m}^3$ for 25% ester content and then increases to $2.3 \pm 0.9 \text{ J/m}^3$ for the 50% ester copolymer. The P3DDT-50E thus behaves very differently than all copolymers studied: it has the lowest modulus combined with a high fracture strain, which makes it a stretchable material with low toughness. The 100% ester polymer (P3ET-100E) was very gooey and not robust enough to make a free-standing film.

The difference in mechanical properties between the P3HT and P3DDT series can be explained by whether the polymers crystallize in one phase or two, as discussed above. In the case of P3HT, the copolymer main chain and side chains are miscible and behave as one phase. As a result, side chain modifications have a large impact on the mechanical properties of P3HT-based copolymers because they also affect the main chain behavior. For the P3DDT series, the main chain and side

chain microphases separate into two phases. As a result, side chain modification has a much smaller impact on the main chain crystallization. This explains why the P3DDT with 10-25% ester content has similar tensile strengths and small fracture strains. Furthermore, the increased toughness with 10% ester content for the P3DDT series is very small compared to that for the P3HT series. The P3DDT-50E behaves very differently from P3DDT, with a much lower modulus, lower tensile strength, and much larger fracture strain. This is consistent with the DSC results for this copolymer.

To investigate the effect of tensile test on film morphology, free-standing films were probed in-house using WAXD before and after they were pulled to failure in tensile tests (data in Figure S41). The WAXD patterns before and after tensile tests were very similar, suggesting that the copolymer film morphology was not altered by stretching. All free-standing films show isotropic rings in WAXD patterns, which are indicative that they do not have a preferred orientation (anisotropic).

Electronic Properties. The electronic properties of P3AT copolymers were evaluated in bottom-gate-top-contact OFETs, and the results are summarized in Table 4 and

Table 4. Summary of OFET Characteristics for the Polymer Films (Average of 8 Devices)

Polymer	$\mu_{\rm h} \ {\rm FET} \ ({\rm cm^2 \ V^{-1} \ s^{-1}})$	$V_{ m th}$ (V)	$I_{ m ON}/I_{ m OFF}$
P3HT (0E)	0.12 ± 0.03	5.3	10^{3}
10E	0.12 ± 0.01	-2.2	10^{4}
20E	$4.2 \pm 1.9 \times 10^{-3}$	-2.8	10^{3}
25E	$2.1 \pm 1.3 \times 10^{-3}$	-7.1	10^{3}
50E	$8.4 \pm 4.6 \times 10^{-4}$	1.8	10^{3}
P3DDT (0E)	$1.3 \pm 0.5 \times 10^{-2}$	13.2	10^{3}
10E	$5.1 \pm 1.2 \times 10^{-2}$	-2.2	10^{4}
20E	$9.8 \pm 9.1 \times 10^{-3}$	-2.6	10^{3}
25E	$7.7 \pm 3.1 \times 10^{-4}$	-8.9	10^{3}
50E	_	_	_
100E	_	_	_

illustrated in Figure 9. All polymers' devices demonstrated OFET behavior in an accumulation mode, and the hole mobility (μ_b) was extracted from the transfer curves using

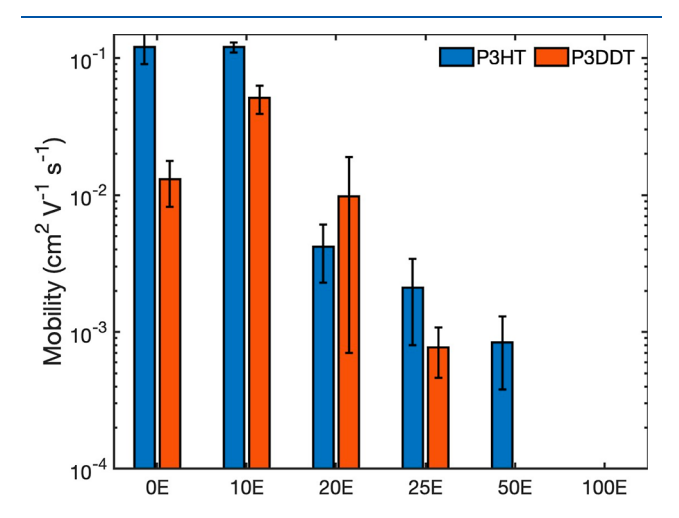


Figure 9. OFET average hole mobility as a function of ester content. $(\mu_{\rm h}^{\rm avg})$.

linear fitting of the ${I_{\rm DS}}^{1/2}$ vs $V_{\rm GS}$ curves in the saturation regime using the following equation: $I_{DS(sat)} = (WC/2L) \mu_{sat} (V_G - V_G)$ $(V_{\rm th})^2$. Notably, no data could be obtained for P3DDT-50 and P3DDT-100E due to poor film formation. For the P3HT series, the μ_h of P3HT was 0.12 \pm 0.03 cm²V⁻¹ s⁻¹, which is excellent for P3HT. Surprisingly, μ_h of the P3HT-10E copolymer was also 0.12 \pm 0.01 cm² V⁻¹ s⁻¹, demonstrating that 10% ester content is not detrimental to charge carrier mobility. Further increasing ester content decreased μ_h , though a μ_h of $\sim 10^{-3}~\text{cm}^2~\text{V}^{-1}~\text{s}^{-1}$ was still maintained for P3HT-20E and P3HT-25E.

Hole mobility for the P3DDT series all have lower μ_h than for the corresponding P3HT copolymers, which is not surprising since the samples are generally more amorphous than P3HT. In addition, hole mobility of longer P3ATs has been shown to be more susceptible to differences in morphology at the dielectric-polymer interface than shorter n-hexyl side chains. 36,37 The μ_h for the P3DDT homopolymer was $1.3 \pm 0.5 \times 10^2$ cm² V⁻¹ s⁻¹. Interestingly, μ_h increased to $5.1 \pm 1.2 \times 10^{-2}$ cm² V⁻¹ s⁻¹ for P3DDT-10E, consistent with the higher relative crystallinity measured for P3DDT-10E than for P3DDT. The μ_h for P3DDT-20E polymer is like that of the P3DDT homopolymer, while that of P3DDT-25E is lower than that of P3DDT. No field-effect could be recorded for P3DDT-50E and P3DDT-100E, partly because of poor film formation. The threshold voltages (V_{th}) and on/off ratios are as expected for P3ATs, though we note that both P3HT-10E and P3DDT-10E have an on/off ratio of 10, which is higher than those of the other polymers.

Film-On-Elastomer. To explore the mechanical properties of thin films, we further tested the best copolymer P3HT-10E using the film-on-elastomer technique and compared it with P3HT of similar MW. The optical images obtained under various percent stretch are shown in Figure 10. The P3HT sample cracked with less than 5% stretch. On the other hand, the P3HT-10E sample does not show any cracks at 5% stretch. Some cracks appear at 10% stretch, and the propagation of the cracks is less extensive than in P3HT, demonstrating that P3HT-10E is more deformable than P3HT.

CONCLUSIONS

Two series of random copolymers with varying amounts of ester functionalized side chains were successfully synthesized and studied. We found large differences in thermal properties, aggregation/morphology, and mechanical properties between the two series. For the P3HT series where the side chains are *n*-hexyl and 6-pentanoatehexyl, the side chains and the main chain crystallize as one phase. As a result, incorporating the ester-functionalized side chain decreases $T_{\rm m}$, $\Delta H_{\rm m}$ and crystallinity and increases the lamellar distance. It also strongly affects mechanical properties, where P3HT-10E was found to be the most mechanically robust, with a toughness of ~90 J/ m³. We attribute the mechanical property improvement to a small increased disorder from the side chain mismatch in the copolymers combined with the ester functionality that can introduce dipole-dipole interactions. The P3HT-10E also maintained a high field-effect mobility of 0.12 cm² V⁻¹ s⁻¹ in thin films, suggesting that the small film morphology changes did not adversely affect the charge transport. Further increasing ester content decreased mobility but was still relatively high with 25% ester. The film-on-elastomer experiment confirmed that thin films of P3HT-10E are more ductile than that of P3HT of similar molecular weight. For the P3DDT series, our

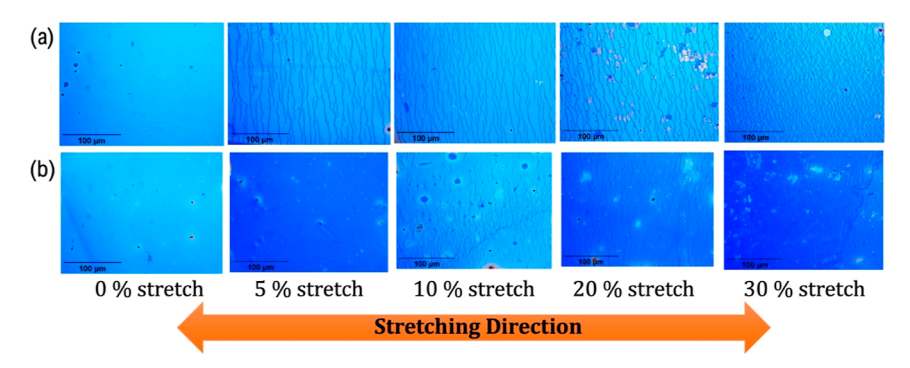


Figure 10. Optical images of (a) P3HT and (b) P3HT-10E on elastomer under various percent stretch. The scale bar is 100 µm.

data are consistent with a microphase separation that is not due to copolymers but due to side chains crystallizing separately from the main chains. Since the n-dodecyl and 6pentanoatehexyl are about the same length, they could cocrystallize together. Because the ester functionality is not in the same phase as the main chain, it does not strongly influence the main chain $T_{\rm m}$ and has a much smaller impact on the mechanical properties for the 10-25% ester content. The P3DDT-10E has the largest toughness of the P3DDT series at ~5 J/m³. In OFETs, the P3DDT-10E has a higher field effect mobility $(0.05 \text{ cm}^2 \text{ V}^{-1} \text{ s}^{-1})$ than P3DDT $(0.01 \text{ cm}^2 \text{ V}^{-1} \text{ s}^{-1})$ due to increased crystallinity. Further adding ester functionality decreases mobility significantly. These results show that tuning the right amount of ester functionalization, especially when the copolymers behave as one phase, is a promising strategy to optimize both charge transport and mechanical robustness of conjugated polymers. These exciting results provide further understanding for the effects of ester-functionalization and side chain length on the mechanical properties of P3ATs.

ASSOCIATED CONTENT

Supporting Information

The Supporting Information is available free of charge at https://pubs.acs.org/doi/10.1021/acs.macromol.3c01886.

Methods and ¹H NMR spectra of monomers and polymers; UV—vis absorbance spectra of as-cast and annealed films; TGA thermograms, summary of thermal properties, calculation of crystallinities, powder WAXD 1D profiles as a function of temperature, and AFM height and phase images; GIWAXD of thin film and WAXD of thick film data; and OFET device output curves (PDF)

AUTHOR INFORMATION

Corresponding Author

Geneviève Sauvé — Department of Chemistry, Case Western Reserve University, Cleveland, Ohio 44106, United States; orcid.org/0000-0002-9721-0447; Email: gxs244@ case.edu

Authors

Quynh D. Tran — Department of Chemistry, Case Western Reserve University, Cleveland, Ohio 44106, United States

Lexi R. Knight — Department of Chemistry, Case Western Reserve University, Cleveland, Ohio 44106, United States

Guanchun Rui — Department of Macromolecular Science and Engineering, Case Western Reserve University, Cleveland, Ohio 44106, United States

Gage T. Mason – Department of Chemistry and Biochemistry, University of Windsor, Windsor, Ontario N9B 3P4, Canada Piumi Kulatunga – Department of Chemistry and Biochemistry, University of Windsor, Windsor, Ontario N9B

Alexander J. Bushnell – Department of Chemistry, Case Western Reserve University, Cleveland, Ohio 44106, United States

Buwei Hou — Department of Chemistry, Case Western Reserve University, Cleveland, Ohio 44106, United States; orcid.org/0009-0003-7288-4116

Lei Zhu — Department of Macromolecular Science and Engineering, Case Western Reserve University, Cleveland, Ohio 44106, United States; orcid.org/0000-0001-6570-9123

Simon Rondeau-Gagné — Department of Chemistry and Biochemistry, University of Windsor, Windsor, Ontario N9B 3P4, Canada; orcid.org/0000-0003-0487-1092

Complete contact information is available at: https://pubs.acs.org/10.1021/acs.macromol.3c01886

Notes

The authors declare no competing financial interest.

ACKNOWLEDGMENTS

3P4, Canada

We thank the National Science Foundation (NSF) CHEM 2203595 and an internal Expanding Horizon grant (Case Western Reserve University) for the financial support. We thank Prof. Stephanie Sydlik at Carnegie Mellon University for measuring the mechanical properties of P3. We also thank Dr. Thumawadee Wongwirat at Case Western Reserve University for the powder WAXD experiments. Thanks to NSF MRI 1334048 for NMR instrumentation and making this work possible. This work was supported by the Natural Sciences and Engineering Research Council of Canada (NSERC) through a Discovery Grants (RGPIN-2022-04428). S.R.-G. also acknowledges the Canada Foundation for Innovation (CFI) and the Ontario Research Fund for the financial support. This research used the 11-BM CMS beamline of National Synchrotron Light Source II (NSLS-II), Brookhaven National Laboratory (BNL), a U.S. Department of Energy User Facility operated for the Office of Science by BNL under contract DE-SC0012704.

REFERENCES

- (1) Skotheim, T. A. Handbook of Conducting Polymers; CRC Press, 1997.
- (2) Günes, S.; Neugebauer, H.; Sariciftci, N. S. Conjugated Polymer-Based Organic Solar Cells. *Chem. Rev.* **2007**, *107* (4), 1324–1338.

- (3) Friend, R. Conjugated polymers. New materials for optoelectronic devices. *Pure Appl. Chem.* **2001**, 73 (3), 425–430.
- (4) Facchetti, A. Semiconductors for organic transistors. *Mater. Today* **2007**, *10* (3), 28–37.
- (5) Zheng, Y.; Zhang, S.; Tok, J. B.; Bao, Z. Molecular Design of Stretchable Polymer Semiconductors: Current Progress and Future Directions. J. Am. Chem. Soc. 2022, 144 (11), 4699–4715.
- (6) Wang, G. J. N.; Gasperini, A.; Bao, Z. Stretchable Polymer Semiconductors for Plastic Electronics. *Adv. Electron. Mater.* **2018**, 4(2)..
- (7) Oh, J. Y.; Bao, Z. Second Skin Enabled by Advanced Electronics. *Adv. Sci. (Weinh)* **2019**, *6* (11), 1900186.
- (8) Baek, P.; Aydemir, N.; An, Y.; Chan, E. W. C.; Sokolova, A.; Nelson, A.; Mata, J. P.; McGillivray, D.; Barker, D.; Travas-Sejdic, J. Molecularly Engineered Intrinsically Healable and Stretchable Conducting Polymers. *Chem. Mater.* **2017**, *29* (20), 8850–8858.
- (9) Dimov, I. B.; Moser, M.; Malliaras, G. G.; McCulloch, I. Semiconducting Polymers for Neural Applications. *Chem. Rev.* **2022**, 122 (4), 4356–4396.
- (10) Ding, Z.; Liu, D.; Zhao, K.; Han, Y. Optimizing Morphology to Trade Off Charge Transport and Mechanical Properties of Stretchable Conjugated Polymer Films. *Macromolecules* **2021**, *54* (9), 3907–3926.
- (11) Root, S. E.; Savagatrup, S.; Printz, A. D.; Rodriquez, D.; Lipomi, D. J. Mechanical properties of organic semiconductors for stretchable, highly flexible, and mechanically robust electronics. *Chem. Rev.* **2017**, *117* (9), 6467–6499.
- (12) Kukhta, N. A.; Luscombe, C. K. Gaining control over conjugated polymer morphology to improve the performance of organic electronics. *Chem. Commun.* (*Camb*) **2022**, 58 (50), 6982–6997.
- (13) Chen, A. X.; Kleinschmidt, A. T.; Choudhary, K.; Lipomi, D. J. Beyond stretchability: Strength, toughness, and elastic range in semiconducting polymers. *Chem. Mater.* **2020**, 32 (18), 7582–7601.
- (14) Liu, D.; Mun, J.; Chen, G.; Schuster, N. J.; Wang, W.; Zheng, Y.; Nikzad, S.; Lai, J. C.; Wu, Y.; Zhong, D.; et al. A Design Strategy for Intrinsically Stretchable High-Performance Polymer Semiconductors: Incorporating Conjugated Rigid Fused-Rings with Bulky Side Groups. J. Am. Chem. Soc. 2021, 143 (30), 11679–11689.
- (15) Xie, R.; Colby, R. H.; Gomez, E. D. Connecting the mechanical and conductive properties of conjugated polymers. *Adv. Electron. Mater.* **2018**, *4* (10), 1700356.
- (16) Cheng, H.-W.; Zhang, S.; Michalek, L.; Ji, X.; Luo, S.; Cooper, C. B.; Gong, H.; Nikzad, S.; Chiong, J. A.; Wu, Y.; et al. Realizing intrinsically stretchable semiconducting polymer films by nontoxic additives. *ACS Mater. Lett.* **2022**, *4* (11), 2328–2336.
- (17) Xu, J.; Wang, S.; Wang, G.-J. N.; Zhu, C.; Luo, S.; Jin, L.; Gu, X.; Chen, S.; Feig, V. R.; To, J. W.; et al. Highly stretchable polymer semiconductor films through the nanoconfinement effect. *Science* **2017**, 355 (6320), 59–64.
- (18) Wu, H. C.; Lissel, F.; Wang, G. J. N.; Koshy, D. M.; Nikzad, S.; Yan, H.; Xu, J.; Luo, S.; Matsuhisa, N.; Cheng, Y.; et al. Metal-Ligand Based Mechanophores Enhance Both Mechanical Robustness and Electronic Performance of Polymer Semiconductors. *Adv. Funct. Mater.* **2021**, 31(11).
- (19) McCullough, R. D. The Chemistry of Conducting Polythiophenes. Adv. Mater. 1998, 10 (2), 93-116.
- (20) Loewe, R. S.; Ewbank, P. C.; Liu, J.; Zhai, L.; McCullough, R. D. Regioregular, Head-to-Tail Coupled Poly(3-alkylthiophenes) Made Easy by the GRIM Method: Investigation of the Reaction and the Origin of Regioselectivity. *Macromolecules* **2001**, *34* (13), 4324–4333.
- (21) Zhang, R.; Li, B.; Iovu, M. C.; Jeffries-El, M.; Sauvé, G.; Cooper, J.; Jia, S.; Tristram-Nagle, S.; Smilgies, D. M.; Lambeth, D. N.; et al. Nanostructure dependence of field-effect mobility in regioregular poly (3-hexylthiophene) thin film field effect transistors. *J. Am. Chem. Soc.* **2006**, *128* (11), 3480–3481.
- (22) Koch, F. P. V.; Rivnay, J.; Foster, S.; Müller, C.; Downing, J. M.; Buchaca-Domingo, E.; Westacott, P.; Yu, L.; Yuan, M.; Baklar,

- M.; et al. The impact of molecular weight on microstructure and charge transport in semicrystalline polymer semiconductors-poly (3-hexylthiophene), a model study. *Prog. Polym. Sci.* **2013**, 38 (12), 1978–1989.
- (23) Smith, Z. C.; Wright, Z. M.; Arnold, A. M.; Sauvé, G.; McCullough, R. D.; Sydlik, S. A. Increased Toughness and Excellent Electronic Properties in Regioregular Random Copolymers of 3-Alkylthiophenes and Thiophene. *Adv. Electron. Mater.* **2017**, 3(1)...
- (24) Wang, C.; Zhang, Z.; Pejić, S.; Li, R.; Fukuto, M.; Zhu, L.; Sauvé, G. High Dielectric Constant Semiconducting Poly(3-alkylthiophene)s from Side Chain Modification with Polar Sulfinyl and Sulfonyl Groups. *Macromolecules* **2018**, *51* (22), 9368–9381.
- (25) Godwin, A. D. 24 Plasticizers. In *Applied Plastics Engineering Handbook*, 2nd ed.; Kutz, M., Ed.; William Andrew Publishing, 2017; pp 533–553.
- (26) You, H.; Jones, A. L.; Ma, B. S.; Kim, G.-U.; Lee, S.; Lee, J.-W.; Kang, H.; Kim, T.-S.; Reynolds, J. R.; Kim, B. J. Ester-functionalized, wide-bandgap derivatives of PM7 for simultaneous enhancement of photovoltaic performance and mechanical robustness of all-polymer solar cells. *J. Mater. Chem. A* **2021**, *9* (5), 2775–2783.
- (27) Wu, Y.-S.; Lin, Y.-C.; Hung, S.-Y.; Chen, C.-K.; Chiang, Y.-C.; Chueh, C.-C.; Chen, W.-C. Investigation of the Mobility-Stretchability Relationship of Ester-Substituted Polythiophene Derivatives. *Macromolecules* **2020**, *53* (12), 4968–4981.
- (28) Bertho, S.; Campo, B.; Piersimoni, F.; Spoltore, D.; D'Haen, J.; Lutsen, L.; Maes, W.; Vanderzande, D.; Manca, J. Improved thermal stability of bulk heterojunctions based on side-chain functionalized poly(3-alkylthiophene) copolymers and PCBM. *Sol. Energy Mater. Sol. Cells* **2013**, *110*, 69–76.
- (29) Campo, B. J.; Bevk, D.; Kesters, J.; Gilot, J.; Bolink, H. J.; Zhao, J.; Bolsée, J. C.; Oosterbaan, W. D.; Bertho, S.; D'Haen, J.; et al. Ester-functionalized poly(3-alkylthiophene) copolymers: Synthesis, physicochemical characterization and performance in bulk heterojunction organic solar cells. *Org. Electron.* **2013**, *14* (2), 523–534.
- (30) Iovu, M. C.; Sheina, E. E.; Gil, R. R.; McCullough, R. D. Experimental Evidence for the Quasi-"Living" Nature of the Grignard Metathesis Method for the Synthesis of Regioregular Poly(3-alkylthiophenes). *Macromolecules* **2005**, *38* (21), 8649–8656.
- (31) Son, S. Y.; Samson, S.; Siddika, S.; O'Connor, B. T.; You, W. Thermocleavage of Partial Side Chains in Polythiophenes Offers Appreciable Photovoltaic Efficiency and Significant Morphological Stability. *Chem. Mater.* **2021**, 33 (12), 4745–4756.
- (32) Guo, Y.; Jin, Y.; Su, Z. Spectroscopic study of the microstructure and phase transition of regioregular poly(3-dodecylthiophene). *Soft Matter* **2012**, *8* (10), 2907–2914.
- (33) Shen, X. B.; Hu, W. G.; Russell, T. P. Measuring the Degree of Crystallinity in Semicrystalline Regioregular Poly(3-hexylthiophene). *Macromolecules* **2016**, *49*, 4501–4509.
- (34) Park, H.; Park, H.; Ahn, H.; Lee, W.; Park, J.; Kim, B. J.; Yoon, D. K. Nanoconfinement-Dependent Chain Orientation of Polymorphs in Poly(3-dodecylthiophene)s. *Chem. Mater.* **2023**, *35* (3), 1355–1362.
- (35) Prosa, T. J.; Winokur, M. J.; McCullough, R. D. Evidence of a Novel Side Chain Structure in Regioregular Poly(3-alkylthiophenes). *Macromolecules* **1996**, 29 (10), 3654–3656.
- (36) Sauvé, G.; Javier, A. E.; Zhang, R.; Liu, J.; Sydlik, S. A.; Kowalewski, T.; McCullough, R. D. Well-defined, high molecular weight poly(3-alkylthiophene)s in thin-film transistors: side chain invariance in field-effect mobility. *J. Mater. Chem.* **2010**, 20 (16), 3195–3201.
- (37) Lee, H. S.; Cho, J. H.; Cho, K.; Park, Y. D. Alkyl Side Chain Length Modulates the Electronic Structure and Electrical Characteristics of Poly(3-alkylthiophene) Thin Films. *J. Phys. Chem. C* **2013**, 117 (22), 11764–11769.